Control of bone resorption in mice by Schnurri-3

Marc N. Wein[a,b], Dallas C. Jones[a], Jae-Hyuck Shim[a], Antonios O. Aliprantis[a,c], Rosalyn Sulyanto[a], Vanja Lazarevic[a], Sandra L. Poliachik[d], Ted S. Gross[d], and Laurie H. Glimcher[a,c,e,f,1,2]

[a]Department of Immunology and Infectious Disease, Harvard School of Public Health, Boston, MA 02115; [d]Department of Orthopedics and Sports Medicine, University of Washington, Seattle, WA 98104; [b]Endocrine Unit, Massachusetts General Hospital, Boston, MA 02114; [c]Division of Rheumatology, Allergy, and Immunology, Department of Medicine, Brigham and Women's Hospital, Harvard Medical School, Boston, MA 02115; [e]Department of Medicine, Harvard Medical School, Boston, MA 02115; and [f]Ragon Institute of Massachusetts Institute of Technology, Massachusetts General Hospital and Harvard University, Charlestown, MA 02129

Mice lacking the large zinc finger protein Schnurri-3 (Shn3) display increased bone mass, in part, attributable to augmented osteoblastic bone formation. Here, we show that in addition to regulating bone formation, Shn3 indirectly controls bone resorption by osteoclasts in vivo. Although Shn3 plays no cell-intrinsic role in osteoclasts, Shn3-deficient animals show decreased serum markers of bone turnover. Mesenchymal cells lacking Shn3 are defective in promoting osteoclastogenesis in response to selective stimuli, likely attributable to reduced expression of the key osteoclastogenic factor receptor activator of nuclear factor-κB ligand. The bone phenotype of Shn3-deficient mice becomes more pronounced with age, and mice lacking Shn3 are completely resistant to disuse osteopenia, a process that requires functional osteoclasts. Finally, selective deletion of Shn3 in the mesenchymal lineage recapitulates the high bone mass phenotype of global Shn3 KO mice, including reduced osteoclastic bone catabolism in vivo, indicating that Shn3 expression in mesenchymal cells directly controls osteoblastic bone formation and indirectly regulates osteoclastic bone resorption.

cAMP response element binding protein | receptor activator of nuclear factor-κB ligand | secondary hyperparathyroidism

Schnurri-3 (Shn3) is a large zinc finger protein belonging to the small group of zinc finger, acid-rich, and serine-threonine rich (ZAS) family proteins (1). Previous in vitro studies have implicated a role for Shn3 in diverse processes, such as Ig gene rearrangement, cell survival, TNF signaling in macrophages, and IL-2 gene expression in helper T lymphocytes (2–6). We recently discovered that mice with germline deletion of Shn3 displayed a massive increase in bone mass, revealing an unexpected role for this protein in the skeletal system (5). Shn3-deficient animals showed markedly augmented osteoblastic bone formation in vivo. Consistently, cultured primary osteoblasts lacking Shn3 express increased levels of classic osteoanabolic genes and produce increased amounts of mineralized ECM. In osteoblasts, Shn3 functions, at least in part, by regulating Runx2 protein levels via its ubiquitination.

A central dogma in skeletal biology is that bone formation and resorption are coupled, such that manipulations that increase bone production by osteoblasts typically increase bone catabolism by osteoclasts (7–9). Pharmacological augmentation of bone production in humans with recombinant parathyroid hormone (PTH) leads to a compensatory increase in serum markers of bone turnover. Likewise, inhibition of bone resorption following bisphosphonate or denosumab treatment leads to decreased bone production (10, 11). In most murine models of increased bone production attributable to osteoblast-intrinsic manipulations, a compensatory increase in osteoclastic activity is typically seen (12, 13). However, this is not always the case (14–16). Although the mechanisms controlling mesenchymal/osteoclast cross-talk are incompletely understood, expression of the crucial osteoclasto-genic factors *TNFSF11* [receptor activator of nuclear factor-κB ligand (RANKL)] and *TNFRSF11B* [osteoprotegerin (OPG)] by chondrocytes, osteoblasts, stromal cells, and osteocytes plays a dominant role (17–19).

Here, we show that in addition to increased bone formation, Shn3-deficient mice display a paradoxical reduction in osteo-clastic bone resorption attributable to an osteoclast-extrinsic mechanism. In addition to producing increased amounts of mineralized ECM, Shn3-deficient stromal/osteoblastic cells are defective in driving osteoclastogenesis in vitro. We show that Shn3 controls expression of RANKL in mesenchymal cells.

Shn3-deficient mice continue to accrue bone with aging even when bone formation rates are no longer elevated. Shn3-deficient mice fail to lose bone in a disuse model of osteolysis. In addition, although deletion of the master regulator of osteo-clastogenesis, NFATc1, increases cortical bone mass in WT mice, it has no effect in the presence of Shn3 deficiency, supporting the contention that Shn3-deficient mice have a marked basal reduction in osteoclastogenesis. Finally, selective mesenchymal deletion of Shn3 with Prx1-Cre recapitulates the observed skeletal phenotype of global Shn3 deletion, including reduced osteoclast numbers and reduced bone catabolism in vivo.

Results

We previously demonstrated that the adult-onset high bone mass phenotype of mice lacking Shn3 persists following WT bone marrow (BM) transplantation, and that Shn3-deficient BM cells display normal osteoclast differentiation and resorptive function in vitro (5). To rule out a role for Shn3 in regulating bone re-sorption in an osteoclast-intrinsic manner further, we performed reciprocal BM transplantation experiments. Good hematopoietic chimerism was achieved (Fig. S1A), and, as expected, the Shn3-deficient high bone mass phenotype mapped to the genotype of the host animal (Fig. S1B). We conclude that Shn3 deficiency exerts its effect on bone mass through its expression in a radio-resistant (i.e., nonosteoclast) cell type in vivo.

Reduced Osteoclast Activity in Shn3-Deficient Mice in Vivo. We sought to characterize osteoclast activity in Shn3$^{-/-}$ mice further in vivo. Because these animals show dramatic elevations in osteo-blast behavior as assayed by dynamic histomorphometry (5), we predicted that these mice might show a compensatory increase in serum markers of bone resorption. This was not the case. As shown in Fig. 1 A and B, serum markers of collagen type 1 cross-linked C-telopeptide (CTX) and Pyd were significantly reduced in young (6-wk-old) Shn3$^{-/-}$ animals compared with WT littermates.

Previously, we reported comparable numbers of osteoclasts in WT and Shn3$^{-/-}$ skeletal tissue as assessed by histomorphometry just below the growth plate in the proximal tibia (5). Given the unexpected decrease in markers of bone resorption, we performed a more extensive histochemical investigation and observed qualitative reductions in osteoclast numbers in whole-mount skull preparations (Fig. 1C) and along the surfaces of increased di-aphyseal trabecular bone (Fig. 1D) in Shn3$^{-/-}$ animals.
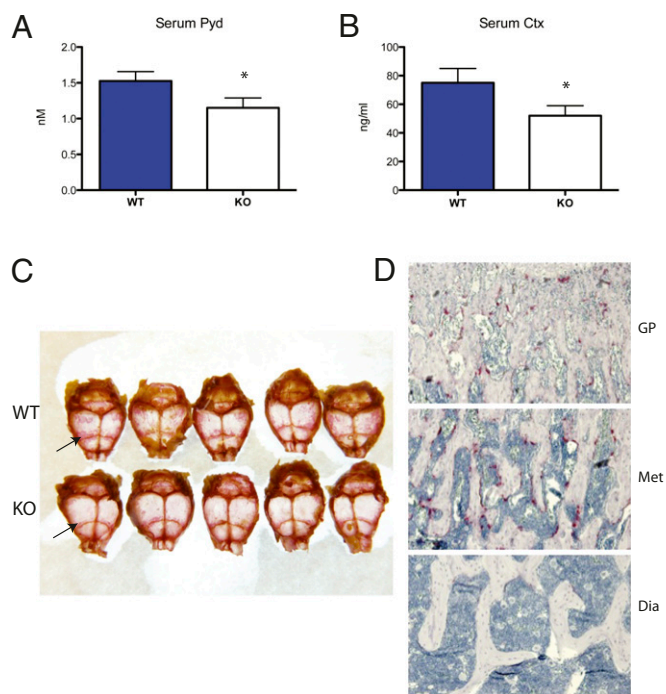
DEVELOPMENTAL BIOLOGY

Fig. 1. Decreased bone resorption in Shn3-deficient mice. (*A*) Serum Pyd levels in 6-wk-old WT and Shn3$^{-/-}$ (KO) animals (*n* = 6 per group). *$P < 0.05$ comparing WT with KO animals. (*B*) Serum CTX levels levels in 6-wk-old WT and KO animals (*n* = 10 per group). (*C*) Representative photograph of whole-mount TRAP stain (pink, arrows highlight prominent staining near sutures) of WT and KO 8-wk-old skull preparations. (*D*) Representative photomicrographs of an 8-wk-old Shn3$^{-/-}$ femur section stained for TRAP (pink) at the growth plate (GP; *Top*), distal metaphyseal (Met; *Middle*), and diaphyseal (Dia; *Bottom*) section levels. (Magnification: 10×.)

Interestingly, this analysis confirmed normal numbers of osteoclasts just below the growth plate in the tibiae and femurs of Shn3$^{-/-}$ animals, suggesting that Shn3 may control osteoclast numbers and/or activity in a skeletal region-selective manner. In Fig. 1*D*, WT control sections were not analyzed because of the drastically different qualitative nature of bone mass and quality at the diaphyseal level. Taken together, these data suggest that Shn3 expression in nonosteoclastic cells may regulate osteoclast development and/or activity.

Mesenchymal Cells Lacking Shn3 Are Defective in Driving Osteoclastogenesis. Radioresistant cells of stromal/osteoblastic lineage are known to support osteoclast development in vitro in response to calciotropic stimuli by expression of RANKL (18–21). To interrogate the ability of Shn3-deficient cells to support osteoclastogenesis, we performed coculture experiments. In these assays, we observed that osteoblastic/stromal cells lacking Shn3 were defective in driving osteoclastogenesis in response to prostaglandin E2 (PGE2) and the β2-adrenergic receptor agonist isoproterenol but not PTH (Fig. 2*A*). We did not specifically address the resorptive capacity of the osteoclasts generated during these in vitro coculture assays. However, we do note that mice lacking Shn3 (Fig. 1 *A* and *B*; see Fig. 5*J*) display reduced serum markers of bone turnover, indicating reduced osteoclast activity in vivo.

Morphological analysis of osteoclasts from these coculture assays revealed a consistent lack of giant multinucleated cells in the presence of Shn3$^{-/-}$ stromal cells (Fig. 2*B*). Consistent with this, RNA obtained from these cocultures showed reduced expression of terminal markers of osteoclast differentiation (cathepsin K and calcitonin receptor) comparing WT with Shn3$^{-/-}$ stromal cells/osteoblasts (Fig. 2*C*).
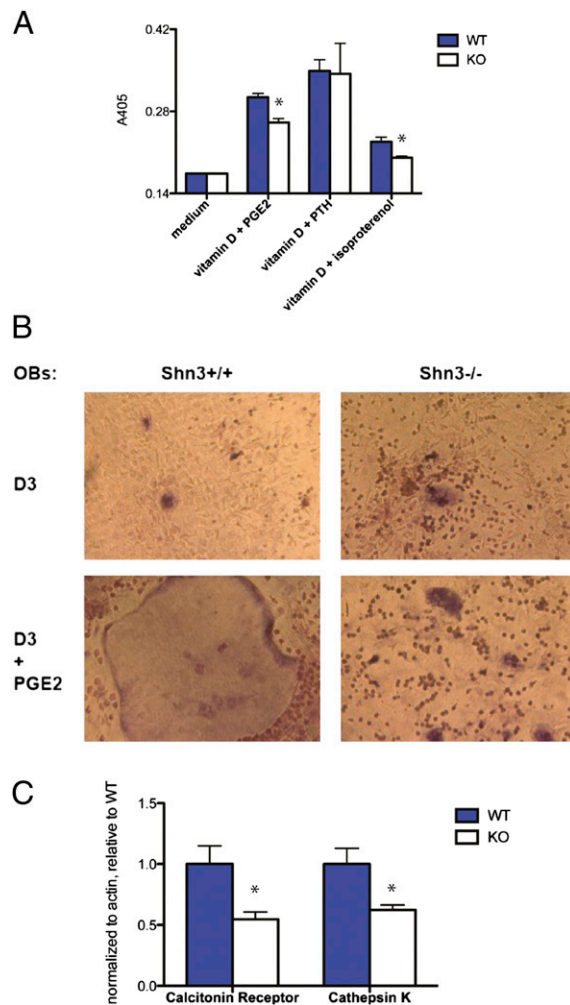

Fig. 2. Shn3-deficient osteoblastic/mesenchymal cells are defective in driving osteoclastogenesis. (*A*) WT or Shn3$^{-/-}$ cells were cocultured with WT BM osteoclast precursors in the presence of the indicated calciotropic agents. After 5 d, tissue culture supernatants were assayed for TRAP activity via colorimetric readout (A405). Error bars represent SD of absorbance from three independent wells. *$P < 0.05$. This experiment was repeated four independent times with similar results. (*B*) Representative photomicrographs of cocultures. (Magnification: 40×.) (*C*) RNA was harvested from cocultures, and expression of calcitonin receptor and cathepsin K was determined by quantitative real-time PCR assay. Levels of the indicated genes were normalized to actin and expressed relative to levels obtained with WT osteoblastic cells. Error bars represent SD of values obtained from PCR triplicate assays. This experiment was repeated three independent times with similar results.

Reduced Levels of RANKL in the Absence of Shn3 in Vivo. We next turned our attention to understanding the mechanism(s) whereby Shn3 expression in osteoblastic/stromal cells might control osteoclast differentiation. To this end, we performed RNA profiling to determine genes controlled by Shn3. In doing so, we found that the critical osteoclastogenic cytokine *TNFSF11* (RANKL) is one such gene whose levels are significantly decreased in Shn3$^{-/-}$ bone tissue (Fig. 3*A*). Serum analysis showed reduced circulating levels of RANKL in Shn3-deficient animals (Fig. 3*B*).

To explore the expression pattern of RANKL in bone tissue lacking Shn3 further, we performed immunohistochemistry for RANKL and histochemical labeling for the osteoclast marker tartrate resistant acid phosphatase (TRAP). These studies demonstrated comparable levels of RANKL in growth plate hypertrophic chondrocytes (Fig. S2*A*) and p10 proximal metaphyseal bone lining cells (Fig. S2*B*) but qualitatively reduced levels of RANKL and TRAP in bone lining cells more distant from the

Fig. 3. Decreased RANKL in Shn3-deficient mice and cells. (A) RNA was isolated from calvariae of WT and Shn3$^{-/-}$ (KO) 8-wk-old mice (n = 5 mice per genotype). Transcript levels of the indicated genes were determined relative to actin by quantitative PCR assay and expressed as normalized to WT. Error bars represent SD values. *P < 0.05. The only gene showing significant change between WT and KO was RANKL. OCN, osteocalcin. (B) Serum RANKL was determined from 8-wk-old WT and KO mice (n = 10 mice per genotype). *P < 0.01. (C) Representative photomicrographs from femurs from 8-wk-old WT and Shn3$^{-/-}$ mice were costained for RANKL immunohistochemistry (IHC) (brown) and TRAP (pink) at the distal metaphysis. (D) Representative diaphyseal sections. Note the paucity of TRAP reactivity and RANKL-immunoreactive cells at this level. (E) Primary calvarial-derived osteoblasts from WT and KO mice were grown in culture for 7 d. RNA was isolated, and transcript levels of RANKL and OPG were determined relative to actin. *P < 0.05. (F) SV40-transformed WT calvarial osteoblast cell line was infected with either control lentivirus, Shn3 shRNA lentivirus, or Shn3 overexpression (N3557) lentivirus. RNA was isolated, and RANKL/OPG levels were determined relative to actin. (G) SV40-transformed WT (clone 20) and Shn3$^{-/-}$ (clone 13) cells were treated with the indicated agent for 90 min, and RANKL RNA levels were determined. (H) Day 0 primary calvarial osteoblasts were treated with the indicated agents for 3 h, and RANKL levels were determined. (Magnification: 10× in C and D.)

growth plate [Fig. 3 *C* (metaphyseal region) and *D* (diaphyseal region)]. Another cell type known to express RANKL is the CD4$^+$ T helper 17 (Th17) cell (22). Shn3 is dispensable for Th17 cell differentiation and RANKL expression (Fig. S2C). Taken together, these data indicate that Shn3 controls RANKL expression by osteoblastic/stromal cells in vivo but not in hypertrophic chondrocytes and Th17 cells.

Reduced Expression of RANKL by Osteoblastic/Stromal Cells Lacking Shn3. Primary calvarial osteoblasts lacking Shn3 show reduced levels of RANKL mRNA after a 7-d in vitro culture period. These cells also display increased levels of the antiosteoclastogenic factor OPG compared with WT cells (Fig. 3E). However, RANKL levels are known to decrease, and OPG levels to increase, during the course of osteoblast differentiation using this in vitro system (23). To circumvent the possibility that the differences observed reflect disparate differentiation states, we acutely altered Shn3 levels in transformed osteoblast cell lines

using lentivirus-based shRNA-mediated gene silencing and overexpression. As shown in Fig. 3F, these manipulations led to the previously observed alterations in RANKL levels but not in OPG levels.

As shown in Fig. 2A, Shn3-deficient osteoblastic cells fully support osteoclastogenesis in response to PTH but not in response to isoproterenol and PGE2. Accordingly, Shn3$^{-/-}$ osteoblastic cells are defective in up-regulating RANKL in response to isoproterenol and PGE2 but not in response to PTH (Fig. 3 *G* and *H*). Acute reductions in Shn3 levels by shRNA-mediated gene silencing reduced responsiveness to PGE2 as expected (Fig. S3A). When coculture experiments were performed in the presence of a neutralizing anti-OPG antibody, the defect in the ability of Shn3$^{-/-}$ osteoblasts to drive osteoclastogenesis was reversed (Fig. S3B), suggesting that reduced RANKL expression by these cells contributes to their inability to support osteoclast differentiation.

Shn3 Controls Expression of RANKL Through cAMP Response Element Binding Protein and an Upstream Regulatory Element. We next sought to determine the mechanism whereby Shn3 controls RANKL expression. *TNFSF11* gene expression is controlled by a variety of distal and proximal regulatory regions (21, 24, 25). We focused on a conserved regulatory region located 76 kb upstream of the transcriptional start site that had been described by two independent groups as important for calciotropic agent responsiveness in vitro and in vivo (26). Shn3 overexpression can enhance activity of this upstream promoter element but not that of the proximal RANKL and OPG gene regulatory regions (Fig. S4A).

Transcription factors, such as vitamin D receptor (VDR), Runx2, cAMP response element binding protein (CREB), and STAT3, are known to associate with this RANKL gene regulatory region (24, 27). We found that Shn3 does not activate transcription from this reporter when the CREB binding sites are deleted (Fig. S4B). In overexpression studies, Shn3 can bind CREB (Fig. S4C) and regulates its transcriptional activity (Fig. S4 D and E). Taken together, these data suggest that Shn3 controls RANKL expression in osteoblastic cells in vivo and in vitro, at least in part, through a mechanism that involves binding to CREB in the context of a conserved upstream regulatory region.

Shn3-Deficient Animals Are Protected from Bone Loss Attributable to Aging and Disuse but Not Secondary Hyperparathyroidism. To explore the functional impact of RANKL regulation by Shn3 further, three models of stimulated bone resorption were used: aging, dietary-induced hypocalcemia, and disuse osteopenia. Young (8-wk-old) Shn3$^{-/-}$ mice show high bone mass associated with an increased rate of bone formation and decreased resorptive markers (5) (Fig. 1 B and C). Interestingly, aged (>3-mo-old) Shn3$^{-/-}$ animals continue to accrue bone, ultimately leading to obliteration of the marrow cavity and extramedullary hematopoiesis (not shown) but display reduced histomorphometric indices of bone formation (Fig. 4A). This phenotype of increasing bone mass with reduced bone formation rates in aged Shn3$^{-/-}$ mice is associated with reduced serum levels of the resorptive markers Pyd and CTX and RANKL (Fig. S5A). These findings suggest that the continued accrual of bone mass in aged Shn3$^{-/-}$ mice is driven by reduced bone resorption. Therefore, it appears that the cause of the high bone mass phenotype in Shn3-deficient mice varies with age. Young mice lacking Shn3 predominantly display an osteoanabolic phenotype, although as the mice age, bone formation slows down and the major phenotype is that of reduced bone resorption. Further studies are required to identify and dissect the age-related switch whereby this transition occurs.

Because PTH was able to increase RANKL expression normally in Shn3-deficient osteoblastic/mesenchymal cells, we wondered whether secondary hyperparathyroidism in vivo would lead to bone loss in Shn3-deficient mice. To test this notion, we placed 11-wk-old WT and Shn3$^{-/-}$ animals on a control diet or a low-calcium diet for 2 wk (28). Shn3$^{-/-}$ mice showed reductions in trabecular bone volume/total volume (BV/TV) (Fig. 4B) and increases in serum markers of bone resorption (Fig. S5B), and were able to maintain normocalcemia (Fig. S5C) in this model. Percent reductions in bone loss comparing WT with Shn3$^{-/-}$ mice were comparable. These data are consistent with our observations that Shn3 is dispensable for PTH-mediated induction of osteoclastogenesis in coculture models (Fig. 2A) and RANKL up-regulation in osteoblastic cells (Fig. 3H). Moreover, these data suggest that the Shn3$^{-/-}$ bone matrix is not "unresorbable," thereby discounting the notion that biomechanical properties alone cause the high bone mass phenotype observed in these mice.

We next used an osteoclast-driven model of disuse osteopenia (29, 30) to test the physiological relevance of our findings further. In this model, botulinum toxin is injected into the hind-limb muscles (quadriceps and/or calf muscle groups), which leads to transient muscle paralysis and subsequent bone loss in the ipsilateral but not contralateral tibia. Both genotypes showed similar
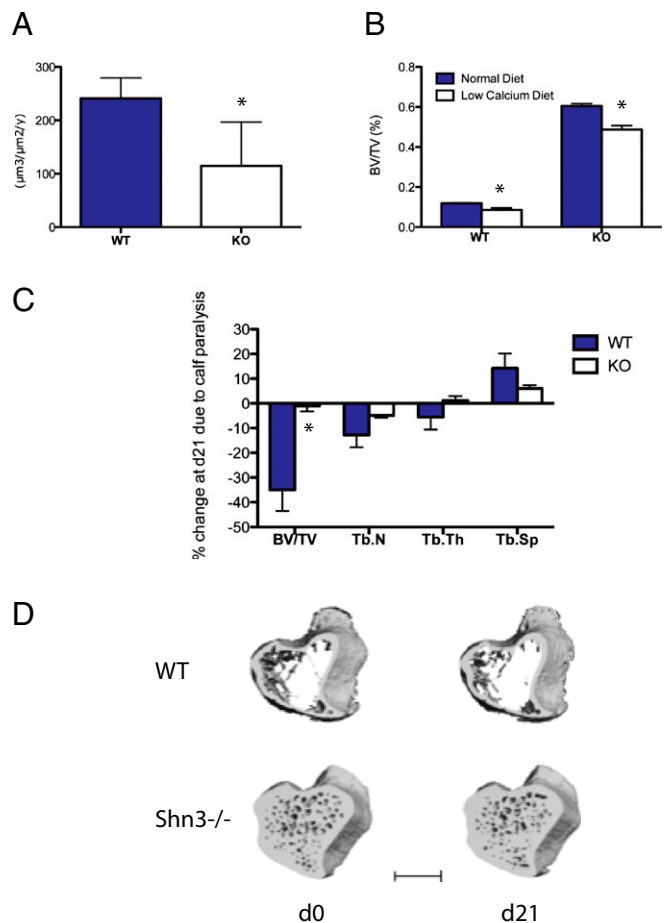

Fig. 4. In vivo analysis of Shn3-deficient mice challenged with resorptive stimuli. (A) Dynamic histomorphometry was performed to quantify bone formation rate in 12-wk-old WT and Shn3$^{-/-}$ (KO) animals (n = 5 mice per group). *P < 0.05. (B) Eleven-week-old WT and Shn3$^{-/-}$ (KO) mice were fed a normal or low-calcium diet for 2 wk. BV/TV in the distal femoral metaphysis was determined by micro computed tomography (μCT) (n = 5 mice per group). (C) Six-month-old WT (n = 6) or Shn3$^{-/-}$ (KO, n = 8) mice were injected with botulinum toxin in the calf muscle. At day 0 (just before toxin injection) and day 21, the indicated parameters were determined by μCT at metaphyseal region of the proximal tibia. Data are expressed as percent change of the indicated parameter attributable to calf paralysis. Tb.N, trabecular number; Tb.Sp, trabecular spacing; Tb.Th, trabecular thickness. (D) Representative μCT images depicting WT and Shn3$^{-/-}$ samples at the level of the proximal tibia during the 21-d study. WT refers to the Shn3 fl/fl genotype, whereas cKO (conditional KO) refers to Shn3 fl/fl × Prx1-Cre animals. (Scale bar: 1 mm.)

muscle atrophy (Fig. S5D). The subset of imaged Shn3$^{-/-}$ animals demonstrated no changes in the contralateral limb attributable to muscle paralysis (−4.2 ± 3.9%) during the 21-d study period. Although WT animals showed expected ipsilateral bone loss following this manipulation, Shn3$^{-/-}$ animals were completely protected at multiple time points (Fig. 4 C and D). This observation further supports a model in which Shn3 plays an important role in regulating bone resorption in response to a variety of physiological stimuli.

Deletion of Osteoclasts Does Not Alter the Diaphyseal High Bone Mass Phenotype in Shn3-Deficient Mice. Because we had observed reduced diaphyseal osteoclast populations in Shn3$^{-/-}$ mice (Fig. 1D), we wondered whether elimination of osteoclasts in the setting of Shn3 deficiency would alter this phenotype in any way. To this end, we intercrossed mice lacking Shn3 with animals harboring a conditional *NFATc1* allele and bearing an Mx1-Cre

(IFN-inducible) transgene (31). In these Shn3/NFATc1 double-KO mice bearing Mx1-Cre transgenes (and control mice lacking both genes individually), NFATc1 deletion at the age of 2 wk was achieved via polyinosinic:polycytidylic acid (poly I:C) injection (31) (*Materials and Methods*). As shown in Fig. S6 *A* and *B*, inducible deletion of NFATc1 (and therefore osteoclasts) led to a significant increase in midshaft BV/TV in WT but not Shn3-deficient mice. These data further indicate that a basal reduction in osteoclastogenesis contributes to the high bone mass phenotype seen in the absence of Shn3.

Reduced Bone Resorption in Mice Lacking Shn3 Only in Mesenchymal Cells. To interrogate further the mechanism whereby Shn3 controls the balance between bone formation and resorption in vivo, we generated mice harboring a *Shn3* allele in which exon 4 is flanked by *loxP* sites (Fig. S7*A*), hereafter called Shn3f/f mice. To determine definitively whether Shn3 expression in mesenchymal cells plays a role in controlling bone resorption, we intercrossed Shn3f/f mice with mice expressing Prx1-Cre, which expresses in the developing mesenchyme of the limbs and skull but not in the axial skeleton (32). Bone RNA harvested showed reduced Shn3 mRNA levels as expected (Fig. S7*B*). Quantitative micro quantitative computed tomography (μQCT) analysis of long bones (femur) from Shn3f/f mice and Shn3f/f mice carrying the Prx1-Cre transgene showed that transgene-carrying animals demonstrated a high bone mass phenotype nearly identical to that of mice lacking Shn3 in all cells (5) (Fig. 5 *A–E*). Vertebrae from Prx1-Cre Shn3f/f mice were identical to those of transgene-negative Shn3f/f mice (data not shown), confirming that Shn3 deletion causes high bone mass through a local (i.e., not humoral) mechanism. Furthermore, femurs from Prx1-Cre Shn3f/f mice

showed improved performance in biomechanical testing compared with transgene-negative controls (Fig. S7 *C–E*).

Histomorphometric analysis was then performed to investigate further the effects of selective Shn3 deletion in mesenchymal cells. As was the case in global Shn3 deletion, removing Shn3 only in Prx1-expressing cells led to a robust increase in bone formation rate (Fig. 5*F*) and serum procollagen type 1 amino-terminal propeptide (P1NP) levels (Fig. 5*G*). In contrast to our previous histomorphometry data from global Shn3-deficient animals, we observed a significant increase in osteoblast numbers when Shn3 was deleted with Prx1-Cre (Fig. 5*H*).

Based on our proposed model that Shn3 deficiency in the mesenchymal lineage leads to a cell-extrinsic reduction in bone catabolism, in part, via reduced RANKL expression, we expected that Prx1-Cre Shn3f/f mice would show reduced osteoclast numbers and activity in addition to increased bone anabolism. Indeed, Prx1-Cre transgene-positive mice showed reduced osteoclast populations via histomorphometry (Fig. 5*I*) and reduced serum CTX levels (Fig. 5*J*). Taken together, these findings further solidify our model that Shn3 expression in mesenchymal cells directly controls osteoblastic bone formation and indirectly regulates osteoclastic bone resorption.

Discussion

We had previously observed that Shn3 functions as an important inhibitor of osteoblastic bone formation (5). Here, we show that the dramatic high bone mass phenotype seen in Shn3-deficient animals is likely attributable to both increased bone formation and reduced bone resorption. Shn3-deficiency seems to uncouple these processes.

Recently, it has been suggested that Shn3 (also known as ZAS3) may play a cell-intrinsic role in regulating osteoclastogenesis by regulating receptor activator of nuclear factor-κB signaling (33). Consistent with our findings, these authors observed increased bone mass with increased fracture resistance in an independent model of germline Shn3 deletion. Similar to our findings, Liu et al. (33) observed decreased numbers of osteoclasts in vivo. However, we believe that our current findings of persistent high bone mass phenotype in WT animals receiving Shn3-deficient BM transplantation (Fig. S1*B*) and, more importantly, a high bone mass phenotype in mice lacking Shn3 selectively in mesenchymal cells (Fig. 5) highlight that the predominant effect of Shn3 deficiency in vivo maps to the mesenchymal, rather than hematopoietic, compartment. Moreover, in our previous experiments (5), we found no defect whatsoever in osteoclast differentiation and function comparing WT and Shn3-deficient BM cells.

It is interesting that Shn3 deficiency leads to qualitative reductions in osteoclasts in calvariae and diaphyseal bone but not in metaphyseal regions. This observation suggests that different cell populations are responsible for RANKL expression and osteoclastogenesis at these different anatomical sites. Indeed, it has previously been suggested that hypertrophic chondrocytes play a critical role in driving the differentiation of metaphyseal osteoclasts/chondroclasts during development, a finding that is consistent with preserved expression of RANKL in these cells in situ in Shn3−/− mice (34, 35). More recently, cell type-specific RANKL deletion has shown that hypertrophic chondrocytes play a major role in regulating metaphyseal osteoclasts (19), whereas late-stage [dentin matrix protein 1 (DMP1)-expressing] osteoblasts/osteocytes are more important sources of RANKL for osteoclasts involved in adult skeletal remodeling (18, 19). Future studies are required to interrogate the activity of Shn3 in DMP1-expressing bone cells.

We found that Shn3 controls RANKL expression, at least in part, through a regulatory region 76 kb upstream of the transcription start site. Just as Shn3 interacts with c-Jun to coactivate AP-1 complexes in the context of the IL-2 gene in T cells (6), Shn3 seems to function as a context-dependent transcriptional coactivator in the setting of the RANKL gene in mesenchymal cells. Little is known about its structure/function relationship, and the mechanism whereby it functions as a transcriptional
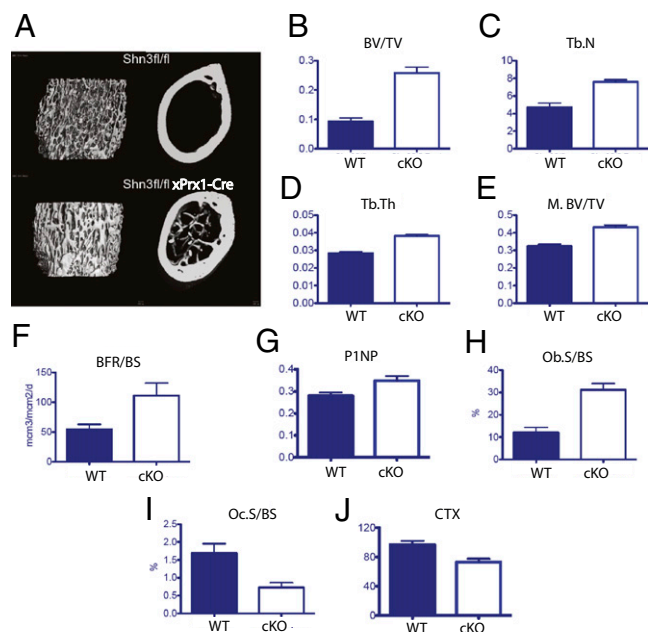

Fig. 5. Deletion of Shn3 in Prx1-expressing cells leads to a high bone mass phenotype with decreased bone catabolism in vivo. (*A*) Representative metaphyseal (*Left*) and midshaft (*Right*) microcomputed tomography (micro-CT) images of mice of the indicated genotype. (*B–D*) Micro-CT–derived metaphyseal BV/TV, trabecular number (Tb.N), and trabecular thickness (Tb.Th) of mice of the indicated genotype. (*E*) Micro-CT–derived diaphyseal (midshaft) BV/TV (M.BV/TV) of mice of the indicated genotype. Osteoblastic parameters in vivo are provided as determined by dynamic (*F*) and static histomorphometry (*H*), as well as serum P1NP levels (*G*). BFR/BS, bone formation rate/bone surface; Ob.S/BS, osteoblast surface/bone surface. Osteoclastic parameters in vivo are determined by static histomorphometry (*I*) and serum CTX levels (*J*). Oc.S/BS, octeoclast surface/bone surface. Comparison of Prx1-Cre transgene-negative and -positive animals for all parameters shown. *P* < 0.05.

coactivator in certain situations. It is interesting that Shn3, like ATF4, is required for RANKL up-regulation in osteoblastic cells in response to isoproterenol but not PTH (36). Future work is required to determine if there is a relationship between Shn3 and ATF4.

Mice lacking Shn3 are completely protected from bone loss induced by muscle paralysis achieved via Botox-induced transient paralysis of calf muscles. Bone loss in this model is osteoclast-driven, as evidenced by complete protection observed in the absence of NFATc1 (30). Although it is clear that osteoclastic bone resorption via RANKL is critical for bone loss in the model, the cellular source of RANKL remains unclear. Recent work suggests that an intercellular communication pathway between osteocytes, RANKL-expressing cells, and osteoclasts involving the secreted protein sclerostin may be involved (37, 38). Mice lacking RANKL in DMP1-expressing cells are protected from bone loss in a similar model (19). Future studies will be required to determine what, if any, role there is for Shn3 in mechanotransduction in osteocytes.

In summary, we have shown that the high bone mass phenotype of Shn3-deficient mice is likely attributable to a combination of increased bone formation and reduced bone resorption. We do note that it is difficult to conclude from our current study which aspect of the Shn3-deficient phenotype (increased bone formation or reduced bone resorption) is more important for the overall high bone mass phenotype. Additional studies are required to address this important outstanding question definitely. That being said, it is provocative that the aged Shn3-deficient mice maintain a dramatic high bone mass phenotype yet show reduced bone formation rates. Based on our findings, one would predict that small-molecule Shn3 inhibitors would increase bone mass through both of these mechanisms.

Materials and Methods

Mice. Shn3-deficient animals were as previously described (5). Conditional Shn3 KO mice were generated at Taconic and on a C57/BL6 background. Prx-1-Cre mice were purchased from the Jackson Laboratory. Conditional NFATc1-deficient mice were as described (31) and intercrossed with Shn3$^{-/-}$ mice.

Serum Measurements. Levels of Pyd (Quidel), CTX (IDS), RANKL (R&D Systems), and calcium (BioAssay) were determined per the instructions of the manufacturers.

Histology and Immunohistochemistry. Decalcified femur sections were stained with RANKL antibodies (sc-7628; Santa Cruz Biotechnology) and TRAP (Sigma).

Osteoblast/Osteoclast Cocultures. Calvarial osteoblasts were grown in medium supplemented only with 10% (vol/vol) FCS and antibiotics. Osteoclast precursors were isolated from adult male BM cells precultured in macrophage-colony stimulating factor (M-CSF) and isolated by Histopaque 1083 (Sigma) gradient centrifugation.

Luciferase Assays and Coimmunoprecipitations. Experiments were performed using previously described methods (5).

In Vivo Muscle Paralysis. Experiments were performed as previously described (29) using 6-mo-old WT and Shn3$^{-/-}$ mice on a BALB/c genetic background. Additional details are provided in *SI Materials and Methods*.

1. Wu LC (2002) ZAS: C2H2 zinc finger proteins involved in growth and development. *Gene Expr* 10:137–152.
2. Wu LC, et al. (1996) The mouse DNA binding protein Rc for the kappa B motif of transcription and for the V(D)J recombination signal sequences contains composite DNA-protein interaction domains and belongs to a new family of large transcriptional proteins. *Genomics* 35:415–424.
3. Allen CE, Mak CH, Wu LC (2002) The kappa B transcriptional enhancer motif and signal sequences of V(D)J recombination are targets for the zinc finger protein HI-VEP3/KRC: A site selection amplification binding study. *BMC Immunol* 3:10.
4. Oukka M, et al. (2002) A mammalian homolog of Drosophila schnurri, KRC, regulates TNF receptor-driven responses and interacts with TRAF2. *Mol Cell* 9:121–131.
5. Jones DC, et al. (2006) Regulation of adult bone mass by the zinc finger adapter protein Schnurri-3. *Science* 312:1223–1227.
6. Oukka M, Kevin MN, Glimcher LH (2004) Schnurri-3 (KRC) interacts with c-Jun to regulate the IL-2 gene in T cells. *J Exp Med* 199:15–24.
7. Erlebacher A, Filvaroff EH, Gitelman SE, Derynck R (1995) Toward a molecular understanding of skeletal development. *Cell* 80:371–378.
8. Matsuo K, Irie N (2008) Osteoclast-osteoblast communication. *Arch Biochem Biophys* 473:201–209.
9. Martin T, Gooi JH, Sims NA (2009) Molecular mechanisms in coupling of bone formation to resorption. *Crit Rev Eukaryot Gene Expr* 19:73–88.
10. Saag KG, et al. (2007) Teriparatide or alendronate in glucocorticoid-induced osteoporosis. *N Engl J Med* 357:2028–2039.
11. Brown JP, et al. (2009) Comparison of the effect of denosumab and alendronate on BMD and biochemical markers of bone turnover in postmenopausal women with low bone mass: A randomized, blinded, phase 3 trial. *J Bone Miner Res* 24:153–161.
12. Elefteriou F, et al. (2006) ATF4 mediation of NF1 functions in osteoblast reveals a nutritional basis for congenital skeletal dysplasiae. *Cell Metab* 4:441–451.
13. Bennett CN, et al. (2007) Wnt10b increases postnatal bone formation by enhancing osteoblast differentiation. *J Bone Miner Res* 22:1924–1932.
14. Li X, et al. (2008) Targeted deletion of the sclerostin gene in mice results in increased bone formation and bone strength. *J Bone Miner Res* 23:860–869.
15. Akune T, et al. (2004) PPARgamma insufficiency enhances osteogenesis through osteoblast formation from bone marrow progenitors. *J Clin Invest* 113:846–855.
16. Sabatakos G, et al. (2000) Overexpression of DeltaFosB transcription factor(s) increases bone formation and inhibits adipogenesis. *Nat Med* 6:985–990.
17. Wada T, Nakashima T, Hiroshi N, Penninger JM (2006) RANKL-RANK signaling in osteoclastogenesis and bone disease. *Trends Mol Med* 12:17–25.
18. Nakashima T, et al. (2011) Evidence for osteocyte regulation of bone homeostasis through RANKL expression. *Nat Med* 17:1231–1234.
19. Xiong J, et al. (2011) Matrix-embedded cells control osteoclast formation. *Nat Med* 17:1235–1241.
20. Takahashi N, et al. (1988) Osteoblastic cells are involved in osteoclast formation. *Endocrinology* 123:2600–2602.
21. O'Brien CA (2010) Control of RANKL gene expression. *Bone* 46:911–919.
22. Sato K, et al. (2006) Th17 functions as an osteoclastogenic helper T cell subset that links T cell activation and bone destruction. *J Exp Med* 203:2673–2682.
23. Thomas GP, Baker SU, Eisman JA, Gardiner EM (2001) Changing RANKL/OPG mRNA expression in differentiating murine primary osteoblasts. *J Endocrinol* 170:451–460.
24. Kim S, Yamazaki M, Zella LA, Shevde NK, Pike JW (2006) Activation of receptor activator of NF-kappaB ligand gene expression by 1,25-dihydroxyvitamin D3 is mediated through multiple long-range enhancers. *Mol Cell Biol* 26:6469–6486.
25. Fu Q, Manolagas SC, O'Brien CA (2006) Parathyroid hormone controls receptor activator of NF-kappaB ligand gene expression via a distant transcriptional enhancer. *Mol Cell Biol* 26:6453–6468.
26. Galli C, et al. (2008) Targeted deletion of a distant transcriptional enhancer of the receptor activator of nuclear factor-kappaB ligand gene reduces bone remodeling and increases bone mass. *Endocrinology* 149:146–153.
27. Kim S, et al. (2007) Multiple enhancer regions located at significant distances upstream of the transcriptional start site mediate RANKL gene expression in response to 1,25-dihydroxyvitamin D3. *J Steroid Biochem Mol Biol* 103:430–434.
28. Aoki K, et al. (2006) A TNF receptor loop peptide mimic blocks RANK ligand-induced signaling, bone resorption, and bone loss. *J Clin Invest* 116:1525–1534.
29. Warner SE, et al. (2006) Botox induced muscle paralysis rapidly degrades bone. *Bone* 38:257–264.
30. Aliprantis AO, et al., Transient muscle paralysis degrades bone via rapid osteoclastogenesis. *FASEB J* 26:1110–1118.
31. Aliprantis AO, et al. (2008) NFATc1 in mice represses osteoprotegerin during osteoclastogenesis and dissociates systemic osteopenia from inflammation in cherubism. *J Clin Invest* 118:3775–3789.
32. Logan M, et al. (2002) Expression of Cre Recombinase in the developing mouse limb bud driven by a Prxl enhancer. *Genesis* 33:77–80.
33. Liu X, et al. (2011) The large zinc finger protein ZAS3 is a critical modulator of osteoclastogenesis. *PLoS ONE* 6:e17161.
34. Masuyama R, et al. (2006) Vitamin D receptor in chondrocytes promotes osteoclastogenesis and regulates FGF23 production in osteoblasts. *J Clin Invest* 116:3150–3159.
35. Usui M, et al. (2008) Murine and chicken chondrocytes regulate osteoclastogenesis by producing RANKL in response to BMP2. *J Bone Miner Res* 23:314–325.
36. Elefteriou F, et al. (2005) Leptin regulation of bone resorption by the sympathetic nervous system and CART. *Nature* 434:514–520.
37. Lin C, et al. (2009) Sclerostin mediates bone response to mechanical unloading through antagonizing Wnt/beta-catenin signaling. *J Bone Miner Res* 24:1651–1661.
38. Tatsumi S, et al. (2007) Targeted ablation of osteocytes induces osteoporosis with defective mechanotransduction. *Cell Metab* 5:464–475.